ACS APPLIED MATERIALS & INTERFACES

Organic Electronic Devices

Synthesis and Characterization of Novel Triarylamine Derivatives with Dimethylamino Substituents for Application in Optoelectronic Devices

Jung-Tsu Wu, Hsiang-Ting Lin, and Guey-Sheng Liou

ACS Appl. Mater. Interfaces, **Just Accepted Manuscript** • DOI: 10.1021/acsami.9b00402 • Publication Date (Web): 29 Mar 2019

Just Accepted

ACS Publications

is published by the American Chemical Society. 1155 Sixteenth Street N.W., Washington, DC 20036

Synthesis and Characterization of Novel Triarylamine Derivatives with Dimethylamino Substituents for Application in Optoelectronic Devices

Jung-Tsu Wu,‡[a] Hsiang-Ting Lin,‡[a] and Guey-Sheng Liou*[a,b]

a. Functional Polymeric Materials Laboratory, Institute of Polymer Science and Engineering, National Taiwan University, 1 Roosevelt Road, 4th Sec., Taipei 10617, Taiwan.

b. Advanced Research Center for Green Materials Science and Technology, National Taiwan University, 10607, Taipei, Taiwan.

KEYWORDS: *electrochromism, electrofluorochromism, ambipolar, triphenylamine, dimethylamino*

ABSTRACT: Two novel triphenylamine-based derivatives with dimethylamino substituents, *N*,*N*'-bis(4-dimethylaminophenyl)-*N*,*N*'-bis(4-methoxyphenyl)-1,4-phenylenediamine (**NTPPA**) and *N*,*N*'-bis(4-dimethylaminophenyl)-*N*,*N*'-bis(4-methoxyphenyl)-1,1'-biphenyl-4,4'-diamine (**NTPB**) were readily prepared for investigating the optical and electrochromic behaviors. These two obtained materials were introduced into electrochromic devices accompany with heptyl viologen (**HV**), and the devices demonstrate high average coloration efficiency of 287 cm^2/C and electrochemical stability. Besides, **NTPB**/**HV** was further used to fabricate electrofluorochromic devices with gel type electrolyte, and exhibit controllable and high PL contrast ratio (I_{off}/I_{on}) of 32.12 from strong emission to truly dark by tuning applied potential in addition to short switching time of 4.9 s and high reversibility of 99% after 500 cycles.

INTRODUCTION

In 1961, Platt reported an interesting phenomenon of electrochromism that the color of materials could be tuned or changed reversibly by gaining or losing electrons during electrochemical process.[1] Then, various electrochromic (EC) materials have been reported and widely applied in our daily life,[2-4] for example, color-changing windows in Boeing 787 Dreamliner and Night Vision Safety mirror products by Gentex. These EC materials can be simply classified into inorganic and organic categories. [5-11] Inorganic materials have been investigated since Deb published the first paper by using EC tungsten oxide in 1969.[12] Comparing to inorganic type materials, organic EC materials can be fabricated into devices with an easier process and lower cost.[13]

Based on the concept of the electrochromism, researchers started to combine it with fluorescence. In the 1990s, some electrochemically monitored fluorescent materials and devices started to pop up.[14] The phenomenon of "electrofluorochromism" mentioned by Rusalov *et al* in 2004,[15] and the first electrofluorochromic (EFC) device was issued by Kim *et al*.[16] Then, many research groups begin to focus on this interesting area.[17-20]

In 2017, Xu et. al published a material with structure of oxadiazole and thiophene units which can turn from emitting neutral state into none-emitting oxidation state.[21] Then, Malik et. al electropolymerized a triphenylamine (TPA) end-capped dendron with EC optical contrast of 68% and EFC PL contrast ratio of 179 during the oxidation switching process.[22] Meanwhile, a gel-type EFC device derived from TPA-containing polyamide has also been fabricated by our group and B. Z. Tang which demonstrate short EFC switching time of <4.9 seconds.[23] TPA-based materials are well known for optoelectronic applications due to the excellent electron-donating nature, easy oxidizability, and hole-transporting ability.[24-26] TPA-containing polymers are easy to acquire high EC performance of optical contrast ratio by tuning the film thickness. However, the response time for switching on and bleaching off would be increased,[27] on the contrary, small molecular materials can effectively avoid such kind of sacrifice.[28,29]

Dimethylamino moieties are often incorporated into the anodic EC materials because of the stronger electron-donating ability than methoxy group. The simplest and most popular material containing dimethylamino groups is *N*,*N*,*N*',*N*'-tetramethyl-1,4-phenylenediamine (TMPD) which has already been investigated in display applications for a long time.[30,31] In 2008, we have also successfully introduced such group into TPA-containing polymer system.[32]

Herein, two novel TPA-based derivatives, *N*,*N*'-bis(4-dimethylaminophenyl)-*N*,*N*'-bis(4-methoxyphenyl)-1,4-phenylenediamine (**NTPPA**) and *N*,*N*'-bis(4-dimethylaminophenyl)-*N*,*N*'-bis(4-methoxyphenyl)-1,1'-

biphenyl-4,4'-diamine (**NTPB**), were prepared in this work, and were used to fabricate the electrochromic devices (ECDs) with heptyl viologen. The obtained devices demonstrate short switching time, high coloration efficiency, and good electrochemical stability. Furthermore, **NTPB** was further incorporated into a gel type EFC device that could control fluorescence intensity from intense emission to truly quench dark state with short response time and excellent reversibility.

EXPERIMENTAL SECTION

Monomer Synthesis. *N,N-Dimethyl-N'-(4-methoxyphenyl)-1,4-phenylendiamine (NDPA).* Tris(dibenzylideneacetone)dipalladium(0) ($Pd_2(dba)_3$, 0.27 g, 0.30 mmol) and tri-tert-butylphosphine ($P(tBu)_3$, 0.14 mL, 0.59 mmol) were added into reactor containing 60 mL anhydrous toluene under nitrogen atmosphere with stirring at room temperature for 10 minutes to undergo the ligand exchange, then *p*-anisidine (2.02 g, 16.5 mmol) was added to the flask sequentially and stirred at 50℃ till the *p*-anisidine dissolved completely. 4-Bromo-*N,N*-dimethylaniline (3.00 g, 15.0 mmol) and sodium *tert*-butoxide (NaO*t*Bu, 11.00 g, 0.11 mol) were added into the solution, and the mixture was stirred at 90℃ for 15 hours, then extracted with ethyl acetate and water till the water layer was cleared. The organic layer was dried over $MgSO_4$ and rotary evaporator. The residual was purified by flash column and recrystallized from hexane to obtain 1.96 g of pale orange crystal (54% yield), mp: 78-79℃. FT-IR (KBr): *v*=3413, 3282, 3035, 2952, 2881, 2834, 2800, 1617, 1513, 1308, 1236, 1037, 813; ^{1}H NMR (400 MHz, DMSO-d_6, δ): 7.28 (s, 1 H, H_d), 6.90-6.84 (m, 4 H, H_{b+c}), 6.78-6.76 (d, 2 H, H_e), 6.69-6.67 (d, 2 H, H_f), 3.66 (s, 3 H, H_a), 2.79 (s, 6 H, H_g).

N,N'-Bis(4-dimethylaminophenyl)-N,N'-bis(4-methoxyphenyl)-1,4-phenylenediamine (NTPPA). Palladium(II) acetate ($Pd(OAc)_2$, 36 mg, 0.16 mmol) and $P(tBu)_3$ (0.036 mL, 0.13 mmol) were added into a 50 mL reactor containing 10 mL anhydrous toluene. **NDPA** (1.53 g, 6.30 mmol), 1,4-dibromobenzene (0.708 g, 3.00 mmol) and NaO*t*Bu (0.96 g, 10.0 mmol) were added into the flask sequentially, and the mixture was refluxed for 4 hours. Then, the mixture was precipitated into methanol after cooling to room temperature, and purified by flash column to obtain 1.04 g of yellow powder (62% yield), mp: 201-203℃ (measured by DSC with the scan rate of 5 ℃/min). FT-IR (KBr): *v*=3037, 2947, 2832, 2796, 1610, 1504, 1239, 1037, 820; ^{1}H NMR (400 MHz, DMSO-d_6, δ): 6.90-6.87 (q, 8 H, H_{b+e}), 6.83-6.81 (d, 4 H, H_c), 6.70-6.67 (t, 8 H, H_{d+f}), 3.70 (s, 6 H, H_a), 2.84 (s, 12 H, H_g); ^{13}C NMR (100 MHz, DMSO-d_6, δ): 154.4 (C_2), 146.9 (C_{11}), 142.1 (C_5), 141.3 (C_6), 137.1 (C_8), 125.9 (C_9), 124.3 (C_3), 122.1 (C_7), 114.6 (C_4), 113.6 (C_{10}), 55.2 (C_1), 40.5 (C_{12}); MS (ESI) m/z: $[M + H]^+$ calcd. for $C_{36}H_{38}N_4O_2$, 558.30; found, 558.30. Anal. calcd for $C_{36}H_{38}N_4O_2$: C 77.39, H 6.86, N 10.03; found: C 76.94, H 6.86, N 9.88.

N,N'-Bis(4-dimethylaminophenyl)-N,N'-bis(4-methoxyphenyl)-1,1'-biphenyl-4,4'-diamine (NTPB). $Pd(OAc)_2$ (36 mg, 0.16 mmol) and $P(tBu)_3$ (0.036 mL, 0.13 mmol) were added into a 50 mL flask containing 10 mL anhydrous toluene. **NDPA** (1.53 g, 6.30 mmol), 4,4'-dibromo-1,1'-biphenyl (0.939 g, 3.00 mmol) and NaO*t*Bu (0.960 g, 10.0 mmol) were added into the container sequentially, and the solution was refluxed for 4 hours. Then, the mixture was precipitated into methanol after cooling to room temperature, and purified by flash column to obtain 1.54 g of light yellow powder (81% yield), mp: 197-201℃ (measured by DSC with the scan rate of 5 ℃/min). FT-IR (KBr): *v*=3033, 2930, 2832, 2797, 1615, 1505, 1492, 1240, 1036, 817; ^{1}H NMR (400 MHz, DMSO-d_6, δ): 7.37-7.35 (d, 4 H, H_e), 7.01-7.00 (d, 4 H, H_b), 6.96-6.94 (d, 4 H, H_f), 6.89-6.88 (d, 4 H, H_c), 6.78-6.76 (d, 4 H, H_d), 6.73-6.71 (d, 4 H, H_g), 3.73 (s, 6 H, H_a), 2.87 (s, 12 H, H_h); ^{13}C NMR (100 MHz, DMSO-d_6, δ): 155.3 (C_2), 147.5 (C_{13}), 147.3 (C_6), 140.4 (C_5), 136.2 (C_{10}), 131.2 (C_9), 126.9 (C_{11}), 126.4 (C_8), 126.0 (C_3), 119.2 (C_7), 114.8 (C_4), 113.6 (C_{12}), 55.2 (C_1), 40.4 (C_{14}) ; MS (ESI) m/z: $[M + H]^+$ calcd. for $C_{42}H_{42}N_4O_2$, 634.33; found, 634.33. Anal. calcd for $C_{42}H_{42}N_4O_2$: C 79.46, H 6.67, N 8.83; found: C 78.90, H 6.90, N 8.89.

RESULT AND DISCUSSION

Synthesis and Basic Characterization of Materials. *N,N*-Dimethyl-*N'*-(4-methoxyphenyl)-1,4-phenylendiamine (**NDPA**) was first synthesized by using Buchwald-Hartwig amination with a yield of 54% from *p*-anisidine and 4-bromo-*N,N*-dimethylaniline.[6] **NDPA** was further reacted with 1,4-dibromobenzene and 4,4'-dibromo-1,1'-biphenyl, respectively, to obtained two new compounds, *N,N'*-bis(4-dimethylaminophenyl)-*N,N'*-bis(4-methoxyphenyl)-1,4-phenylenediamine (**NTPPA**) and *N,N'*-bis(4-dimethylaminophenyl)-*N,N'*-bis(4-methoxyphenyl)-1,1'-biphenyl-4,4'-diamine (**NTPB**) with the yield of 62 and 81%. The synthetic routes are summarized in **Scheme 1**. The structures of these two new compounds were firstly compared with **NDPA** by using FT-IR as shown in Figure S1 and S2. According to the spectra, the peaks at the range of 3000-2700 cm^{-1} belong to the C-H stretching, while the N-H stretching of **NDPA** in the range of 3470-3130 cm^{-1} disappeared for **NTPPA** and **NTPB**. The more detail confirmation of the structures was

Scheme 1. Synthesis Routes of the Materials

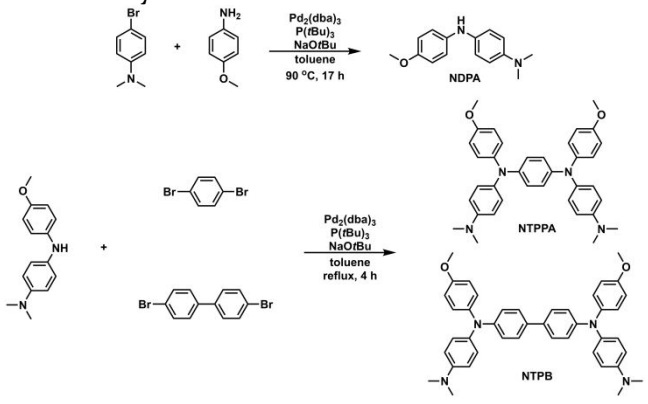

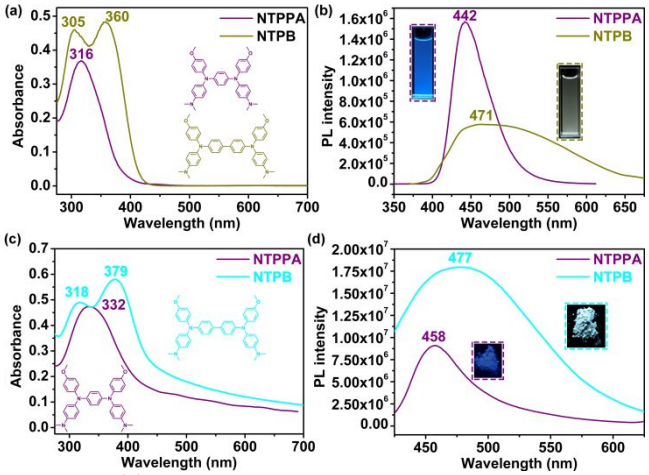

Figure 1. (a) Absorption spectra of **NTPPA** and **NTPB** in DMSO solution. (b) PL spectra of **NTPPA** and **NTPB** in DMSO solution. (Solution concentration: 10 μM) (c) Absorption spectra of **NTPPA** and **NTPB** in solid state. (d) PL spectra of **NTPPA** and **NTPB** in solid state.

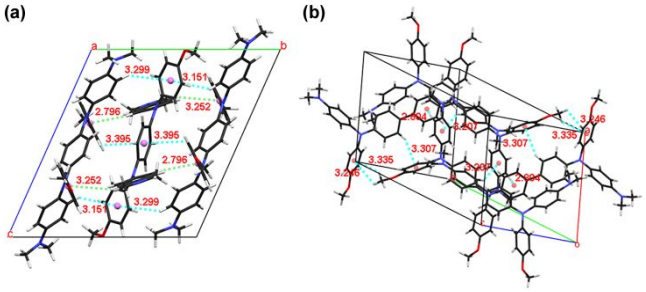

Figure 2. Single crystal packing diagrams and CH/π interaction of (a) **NTPPA** and (b) **NTPB** in a unit cell.

demonstrated by the NMR measurement, and the results are depicted in Figure S3-S11.

Optical and Electrochromic Behaviors. The UV-vis absorption and photoluminescence (PL) behaviors of these materials were investigated in dilute solution (10 μM) of dimethyl sulfoxide (DMSO) and solid state at room temperature, and the results are listed in **Table 1**. Both **NTPPA** and **NTPB** reveal absorption bands at 316 and 360 nm in DMSO solution as shown in **Figure 1a**, and the corresponding PL spectra display maximum bands at 442 and 471 nm as shown in **Figure 1b**, respectively. **Figure 1c** and **1d** exhibit the UV-vis absorption and PL spectra of the same materials in the solid state, showing absorption peaks at 332 and379 nm, and PL emission peaks at 458 and 477 nm, respectively.

Based on the results depicted in **Figure 1** and **Table 1**, **NTPB** demonstrates an AIE property with α_{AIE} of 17.4 calculated from the quantum yield at the solid state of 29.5% and DMSO solution of 1.7%. According to the single crystal packing diagrams illustrated in **Figure 2**, **NTPPA** containing three molecules in every unit cell exists several CH/π interaction each other with distance from 2.796 to 3.395 Å, while **NTPB** shows CH/π interaction only between every two molecules with the distance from 2.804 to 3.335 Å. Consequently, the energy of **NTPPA** can

Table 1. Optical properties of TPA-based materials.

	Solution			Powder		
	λ_{max}^{abs} [nm]	λ_{max}^{em} [nm][a)]	Φ_{PL} [%][b)]	λ_{max}^{abs} [nm]	λ_{max}^{em} [nm][a)]	Φ_{PL} [%][c)]
NTPPA	316	442	2.6	332	458	2.2
NTPB	360	471	1.7	379	477	29.5

[a] Both of λ_{max}^{em} were excited at λ_{max}^{abs}.
[b] The quantum yield was measured by using quinine sulfate as a standard at 25°C(concentration of 10 μM in 1 N H_2SO_4, assuming photoluminescence quantum efficiency of 0.546).
[c] PL quantum yields of solid-state molecules were determined by using a calibrated integrating sphere.

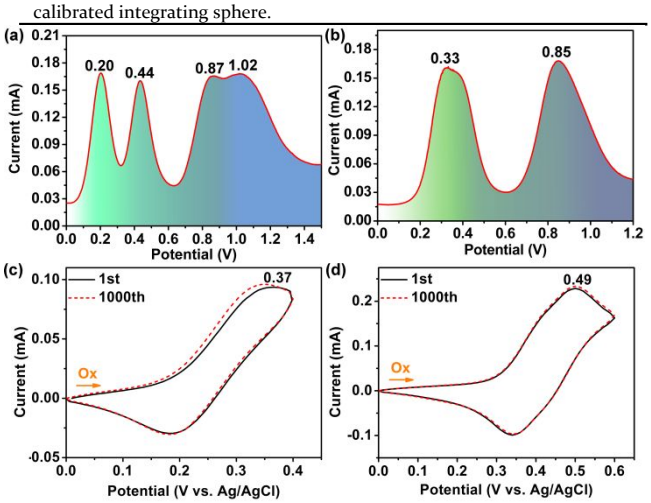

Figure 3. Differential pulse voltammograms of (a) **NTPPA** and (b) **NTPB** conducted with platinum net in 0.1 M $TBABF_4$/GBL at the scan rate of 2 mV/s, pulse width of 25 ms, and pulse period of 0.2 s, and pulse amplitude of 50 mV. Continuous cyclic voltammograms of (c) **NTPPA** and (d) **NTPB** conducted with ITO-coated glass in 0.1 M $TBABF_4$/ at a scan rate of 50 mV/s. (Materials concentration: 1.0×10^{-3} M)

transfer between every three molecules but **NTPB** can only transfer between every two molecules, resulting in lower quantum yield for **NTPPA** in the solid state.

The electrochemical behavior of these two novel EC materials was investigated by differential pulse voltammetry (DPV) using a quartz cell with a platinum net as the working electrode in anhydrous γ-butyrolactone (GBL) containing 1 mM of the EC materials and 0.1 M of tetra-*n*-butylammonium tetrafluoroborate ($TBABF_4$) as the supporting electrolyte under the nitrogen atmosphere for oxidation measurement, respectively. **Figure 3a** and **3b** depict the DPV diagrams of the obtained EC materials. **NTPPA** showed four oxidation peaks at 0.20, 0.44, 0.87 and 1.02 V, corresponding to the number of electroactive nitrogen centers, while only two main oxidation peaks for **NTPB** could be observed at 0.33 V and 0.85 V ascribed to the other two oxidation stages were embedded into the main peaks due to too similar potentials to be distinguished. In addition, both of the EC materials reveal excellent electrochemical stability confirmed by cyclic

voltammetry (CV) with a continuous 1000 cycles scanning at

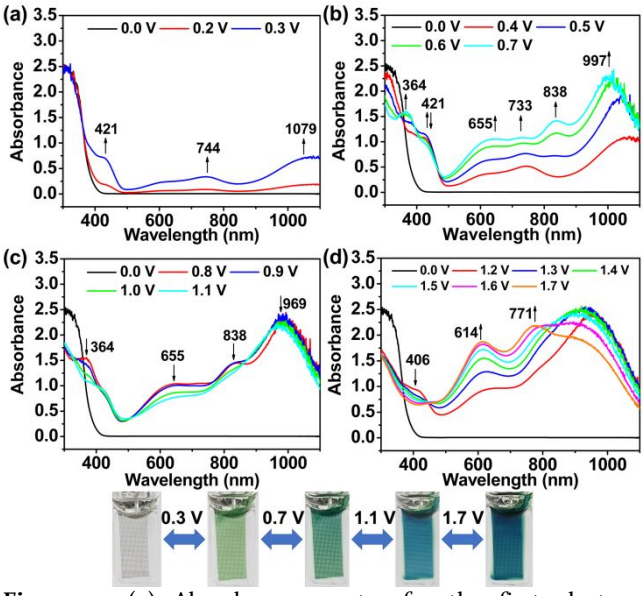

Figure 4. (a) Absorbance spectra for the first electron oxidation of **NTPPA** at the applied potential from 0.2-0.3 V. (b) For the second electron oxidation of **NTPPA** at the applied potential from 0.4-0.7 V. (c) For the third electron oxidation of **NTPPA** at the applied potential from 0.8-1.1 V. (d) For the fourth electron oxidation of **NTPPA** at the applied potential from 1.2-1.7 V. **NTPPA** (1 mM) was dissolved in 0.1 M $TBABF_4$/PC.

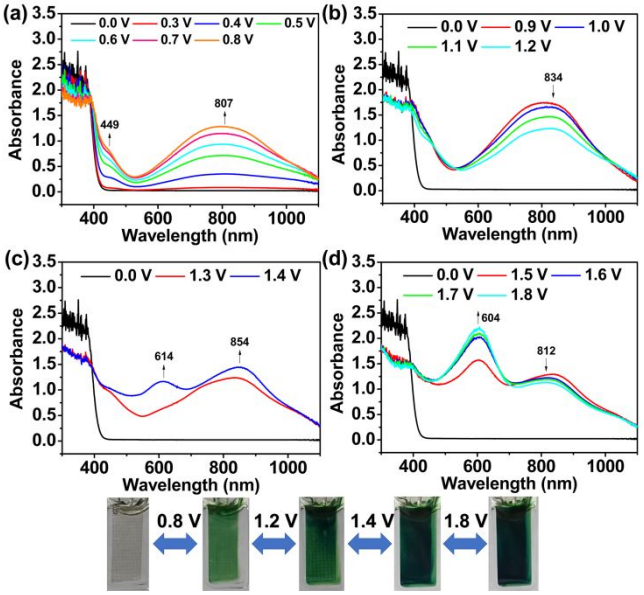

Figure 5. (a) Absorbance spectra for the first electron oxidation of **NTPB** at the applied potential from 0.0-0.8 V. (b) For the second electron oxidation of **NTPB** at the applied potential from 0.9-1.2 V. (c) For the third electron oxidation of **NTPB** at the applied potential from 1.3-1.4 V. (d) For the fourth electron oxidation of **NTPB** at the applied potential from 1.5-1.8 V. **NTPB** (1 mM) was dissolved in 0.1 M $TBABF_4$/PC.

their first oxidation state as depicted in **Figure 3c** and **3d**, respectively.

Spectroelectrochemistry. The spectroelectrochemical measurement was used to demonstrate EC characteristics of these materials by using an optically transparent thin-layer electrode (OTTLE) coupled with UV-vis spectroscopy. The typical absorption spectra and the correspondingEC coloring behaviors of **NTPPA** and **NTPB** are shown in **Figure 4** and **Figure 5**. As shown in **Figure 4a**, three new characteristic absorption peaks at 421, 744 and 1079 nm appear simultaneously for **NTPPA** during oxidation at 0.0-0.3 V. The absorption at the near-IR region could be ascribed to the inter-valence charge transfer (IV-CT) excitation caused by the electron coupling between neutral nitrogen and cation radial nitrogen centers via the phenyl bridge.[25,26] When higher potential (0.4-0.7 V) was applied to the second oxidation state, the characteristic absorbance peak at the UV region started to decrease, while the intensity of peaks at 744 nm and IVCT band increases and shifts to 733 and 997 nm, respectively. Besides, three new peaks emerge at 364, 655, and 838 nm as shown in **Figure 4b**. The third oxidation of the **NTPPA** (0.8-1.1 V, **Figure 4c**) displays no obvious absorption change. For the last oxidation state of **NTPPA** as depicted in **Figure 4d**, two new peaks arise up at 614 and 771 nm with higher absorbance. The color of **NTPPA** could be tuned from green to blue by gradually increasing the applied potential. For **NTPB**, the characteristic absorption peaks at 449 and 807 nm show up gradually during the formation of the first cationic radical state (0.0-0.8 V) as shown in **Figure 5a**. When applied potential increased to 0.9-1.2 V for the second oxidation state, the broadband at 807 nm decreased and shifted to 834 as depicted in **Figure 5b**. For the third oxidation state of **NTPB** shown in **Figure 5c**, two new peaks at 614 and 854 nm grew up, then the peak at 614 nm shifted to 604 with enhanced absorbance, while the peak at 854 nm decreased and shifted to 812 nm in the fourth oxidation state (**Figure 5d**).

Electrochemical and Electrochromic Behaviors of the ECDs. The electrochemical properties for the ambipolar liquid-type ECDs derived from **NTPPA**/**HV** and **NTPB**/**HV** in anhydrous GBL were investigated by CV, respectively. The first oxidation state was chosen for further studies, and the oxidation peaks at 0.71 V and 0.92 V for **NTPPA**/**HV** and **NTPB**/**HV** are shown in **Figure 6a** and **6b**. Furthermore, the spectroelectrochemical study of

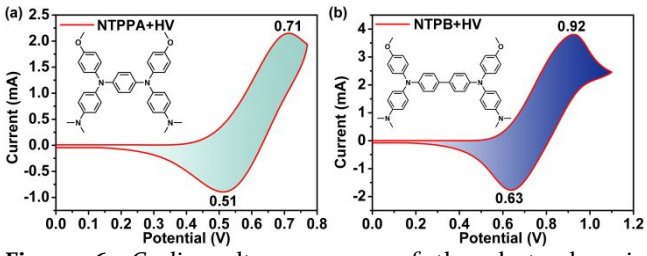

Figure 6. Cyclic voltammograms of the electrochromic devices derived from (a) **NTPPA**/**HV** and (b) **NTPB**/**HV** at the scan rate of 50 mV/s. Device is ITO glass with 2×2 cm^2 active

area containing 0.015/0.015 M of **NTPPA/HV** or **NTPB/HV** in about 0.05 mL of GBL.

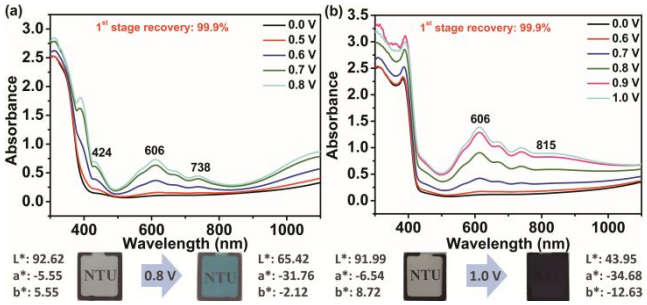

Figure 7. Absorbance spectra and the corresponding electrochromism of the electrochromic device derived from (a) **NTPPA/HV** at the applied potential from 0.0-0.8 V and (b) **NTPB/HV** at the applied potential from 0.0-1.0 V. Device is ITO glass with 2×2 cm² active area containing 0.015/0.015 M of **NTPPA/HV** or **NTPB/HV** in about 0.05 mL of GBL.

these ambipolar ECDs based on **NTPPA/HV** and **NTPB/HV** was also conducted. The typical UV-vis absorption spectra and the corresponding EC coloring behaviors for the first oxidation state of **NTPPA/HV** and **NTPB/HV** are shown in **Figure 7**. The change of the absorption spectra for **NTPPA/HV** at different working potential from 0.0 to 0.8 V shown in **Figure 7a** reveals three absorption peaks (424, 606 and 738 nm) in the visible light region and one in the near-IR region. The color changed from colorless (L*: 92.62, a*: -5.55, b*: 5.55) to a pale-blue color (L*: 65.42, a*: -31.76, b*: -2.12) with the reversibility of 99.9%. For the device of **NTPB/HV**, when the applied potential was given from 0.0 to 1.0 V, two peaks in the visible light region (449 and 606 nm) and one in the near-IR region grew up as shown in **Figure 7b**, with the color change from colorless (L*: 91.99, a*: -6.54, b*: 8.72) to a dark blue-green color (L*: 43.95, a*: -34.68, b*: -12.63) and 99.9% reversibility.

Electrochromic Switching and Stability of the ECDs. The electrochromic switching study of the obtained ECDs could be applied for recording the difference of the optical transmittance as a function of time and calculating the response time by stepping potential between the bleaching and coloring states repeatedly. Switching data of the devices based on the corresponding materials are summarized in **Figure 8** and Figure S12. The definition of the switching time is the time at the 90% of the full switched in transmittance as the result of the difficulty for the human eye to perceive any further color change beyond such percentage. As delineated in **Figure 8a**, the device derived from **NTPPA/HV** exhibits average switching time of 3.8 s for the coloring process (0.8 V) and 4.4 s for the bleaching process (-0.1 V). On the other hand, the device based on **NTPB/HV** demonstrates average switching time of 4.2 s for the coloring process (1.0 V) and 6.9 s for the bleaching process (-0.1 V) as depicted in **Figure 8b**. In addition, to identify the electrochemical performance of the ECDs, coloration efficiency (CE=$\Delta OD/\Delta Q$) will be an essential factor. CE describes the change in the optical density (OD=log(T_b/T_c)) per unit of charge density (Q/A: amount of the charge (Q) consumed per unit of working

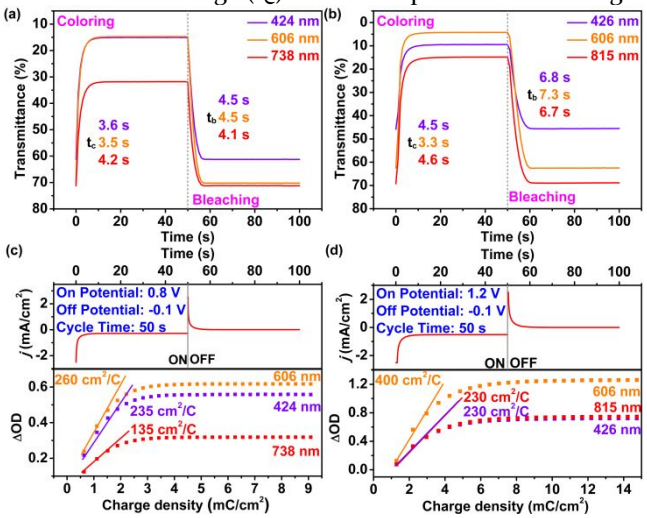

Figure 8. Electrochromic switching response at the relative wavelength of the electrochromic device derived from (a) **NTPPA/HV** between 0.8 V (coloring) and -0.1 V (bleaching) and (b) **NTPB/HV** between 1.0 V (coloring) and -0.1 V (bleaching). Current consumption and change in the in-situ optical density vs. the charge density of the electrochromic device based on (c) **NTPPA/HV** between 0.8 V (coloring) and -0.1 V (bleaching) and (d) **NTPB/HV** between 1.0 V (coloring) and -0.1 V (bleaching). Device is ITO glass with 2×2 cm² active area containing 0.015/0.015 M of **NTPPA/HV** or **NTPB/HV** in about 0.05 mL of GBL.

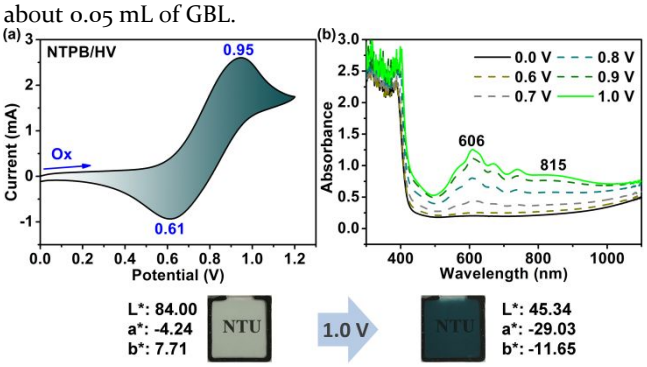

Figure 9. (a) Cyclic voltammogram (scan rate: 50 mV/s) and (b) absorbance spectra (applied potential: 0.0-1.0 V) of the electrofluorochromic device derived from **NTPB/HV** with gel-type electrolyte. Device is ITO glass with 2×2 cm² active area containing 0.015/0.015 M of **NTPB/HV** in about 0.05 mL of GBL.

area (A)) throughout the switching process. The changes of optical density at the related absorption wavelength versus injected charge density at the corresponding potentials are plotted in **Figure 8c** and **Figure 8d**. The numerical values of CE could be obtained from the slopes of tangent lines which match with the linear segment of the curves. The average CE of devices from **NTPPA/HV** is 210 cm²/C and **NTPB/HV** is 287 cm²/C. Furthermore, the EC stability of these devices was also evaluated by measuring the optical absorption change after 1000

switching cycles, confirming excellent stability with only 0.5% and 1.7% decay in transmittance for the devices derived from **NTPPA**/**HV** and **NTPB**/**HV**, respectively.

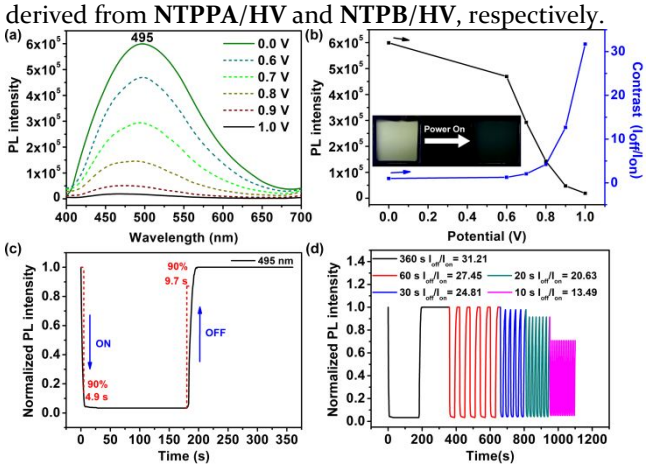

Figure 10. (a) PL spectra, (b) Potential vs PL and contrast diagram, (c) fluorescence switching responses and (d) switching time test of gel-type EFCD derived from **NTPB**/**HV**. Switching time test was measured at different step cycle times of 360, 60, 30, 20, and 10 s by applying voltage between -0.1 and 1.0 V.

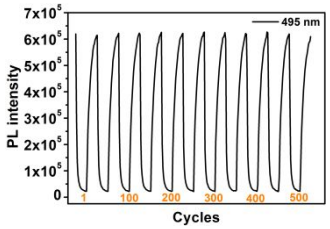

Figure 11. Repetitive switching time test of EFCD based on **NTPB**/**HV** between 1.0 V (on) and -0.1 V (off) with cycle time of 15 s.

Electrochemical and Electrochromic Behaviors of the EFCDs. **NTPB**/**HV** was further fabricated into Electrofluorochromic device (EFCD) with a gel-type electrolyte. The electrochemical and EC results of the EFCD shown in **Figure 9** reveal the first oxidation potential at 0.95 V approximate to those of ECDs mentioned above. The device demonstrates color change from the transparent neutral form with L*a*b* values (84.00, -4.24, and 7.71) to blue-green oxidized state with L*a*b* values (45.34, -29.03, and -11.65) at the applied voltage of 1.0 V.

Electrofluorochromic Behavior of the EFCD. The obtained EFCD shows a PL emission maximum (λ_{em}) at 495 nm, and the fluorescence intensity could be tuned with the applied potentials as shown in **Figure 10a** and **10b**. Since the applied voltage increased from 0.0 to 1.0 V, the fluorescence of **NTPB**/**HV** could be almost extinguished owing to the formation of **NTPB** cation radical, resulting in high PL contrast ratio (I_{off}/I_{on}) of 31.21. The **EFCD** could return to its original fluorescence state after removing the applied potential which means it exhibits electrochemically invertible fluorescence switching behavior between neutral (fluorescent) state and oxidized (non-fluorescent) state by a repetitious applied voltage. **Figure 10c** displays the fluorescence switching time estimated at 90% of the full switching of **NTPB**/**HV** which was monitored at 495 nm with 4.9 and 9.7 seconds for switching on and off, respectively. Besides, the response time-dependent behavior of PL contrast ratio as depicted in **Figure 10d** reveals contrast ratio ranging from 31.21 to 13.49 for **NTPB**/**HV** device when the switching cyclic time was reduced from 360 seconds to 10 seconds. Furthermore, **Figure 11** exhibits long-term stability and reversibility of the EFCD obtained by setting the PL intensity as a function of switching cycles, demonstrating high reversibility of 99% after 500 cycles for the EFCD derived from **NTPB**/**HV**.

CONCLUSION

Two novel monomeric dimethylamine-containing triphenylamine-based EC materials, **NTPPA** and **NTPB**, were readily prepared from Buchwald-Hartwig amination and were further fabricated into ECDs. The dimethylamino substituents not only provide stronger electron-donating ability than the methoxy groups but also multiply the oxidation states comparing to their original structure. The modification can effectively lower their oxidation potential and further reduce the power consumption that makes them more suitable to be utilized as green energy materials. The ECDs derived from these materials accompanying with HV demonstrate good EC stability with short switching time. Furthermore, **NTPB** was also confirmed to be a suitable material for the EFC application. The obtained EFC device also demonstrates high PL contrast ratio (I_{off}/I_{on}), excellent stability and short switching time, implying great potential of **NTPB** in the optoelectronic application.

ASSOCIATED CONTENT

The Supporting Information is available free of charge on the ACS Publications website at DOI: .
Experimental section (materials and method). ^{1}H, ^{13}C, H-H COSY, C-H HSQC NMR spectra, FT-IR, basic EC properties and single crystal data of materials. (PDF)

AUTHOR INFORMATION

Corresponding Author

* E-mail: gsliou@ntu.edu.tw (G. S. Liou)

ORCID

Guey-Sheng Liou: 0000-0003-3725-3768
Jung-Tsu Wu: 0000-0001-5523-1509

Present Addresses

Functional Polymeric Materials Laboratory, Institute of Polymer Science and Engineering, National Taiwan University, 1 Roosevelt Road, 4th Sec., Taipei 10617, Taiwan.

Author Contributions

‡Jung-Tsu Wu and Hsiang-Ting Lin contributed equally.

ACKNOWLEDGMENT

This work was financially supported by the Advanced Research Center of Green Materials Science and Technology from The Featured Area Research Center Program within the framework of the Higher Education Sprout Project by the Ministry of Education (107L9006) and the Ministry of Science and Technology in Taiwan (107-3017-F-002-001 and 107-2113-M-002-024-MY3).

REFERENCES

(1) Platt, J. R. Electrochromism, a Possible Change of Color Producible in Dyes by an Electric Field. *J. Chem. Phys.* **1961**, *34*, 862-863.
(2) Azens, A.; Granqvist, C. G. Electrochromic Smart Windows: Energy Efficiency and Device Aspects. *J. Solid State Electrochem.* **2003**, *7*, 64-68.
(3) Yang, P. H.; Sun, P.; Mai, W. J. Electrochromic Energy Storage Devices. *Mater. Today,* **2016**, *19*, 394-402.
(4) Wang, Y.; Runnerstrom, E. L.; Milliron, D. J. Switchable Materials for Smart Windows. Annu. Rev. Chem. Biomol. Eng. **2016**, *7*, 283-304.
(5) Dautremontsmith, W. C. Transition-Metal Oxide Electrochromic Materials and Displays - a Review .1. Oxides with Cathodic Coloration. *Displays*, **1982**, *3*, 3-22.
(6) DeLongchamp, D. M.; Hammond, P. T. High-Contrast Electrochromism and Controllable Dissolution of Assembled Prussian Blue/Polymer Nanocomposites. *Adv. Funct. Mater.* **2004**, *14*, 224-232.
(7) Weng, D.; Shi, Y. C.; Zheng, J. M.; Xu, C. Y. High Performance Black-to-Transmissive Electrochromic Device with Panchromatic Absorption Based on TiO2-Supported Viologen and Triphenylamine Derivatives. *Org. Electron.* **2016**, *34*, 139-145.
(8) Beaujuge, P. M.; Reynolds, J. R. Color Control in π-Conjugated Organic Polymers for Use in Electrochromic Devices. *Chem. Rev.* **2010**, *110*, 268-320.
(9) Neo, W. T.; Ye, Q.; Chua, S. J.; Xu, J. W. Conjugated Polymer-Based Electrochromics: Materials, Device Fabrication and Application Prospects. *J. Mater. Chem. C* **2016**, *4*, 7364-7376.
(10) Huang, D. C.; Wu, J. T.; Fan, Y. Z.; Liou, G. S. Preparation and Optoelectronic Behaviours of Novel Electrochromic Devices Based on Triphenylamine-Containing Ambipolar Materials. *J. Mater. Chem. C* **2017**, *5*, 9370-9375.
(11) Laschuk, N. O.; Ebralidze, I. I.; Poisson, J.; Egan, J. G.; Quaranta, S.; Allan, J. T. S.; Cusden, H.; Gaspari, F.; Naumkin, F. Y.; Easton, E. B.; Zenkina, O. V. Ligand Impact on Monolayer Electrochromic Material Properties. ACS Appl. Mater. Interfaces, **2018**, *10*, 35334-35343.
(12) Deb, S. K. A Novel Electrophotographic System. *Appl. Opt.* **1969**, *8*, 192-195.
(13) Nguyen, W. H.; Barile, C. J.; McGehee, M. D. Small Molecule Anchored to Mesoporous ITO for High-Contrast Black Electrochromics. *J. Phys. Chem. C* **2016**, *120*, 26336-26341.
(14) Resch-Genger, U.; Hennrich, G. Fluorescent Redox-Switchable Devices. *Top. Fluoresc. Spectrosc.* **2005**, *9*, 189-218.
(15) Rusalov, M. V.; Druzhinin, S. I.; Uzhinov, B. M. Intramolecular Fluorescence Quenching of Crowned 7-Aminocoumarins as Potential Fluorescent Chemosensors. *J. Fluoresc.* **2004**, *14*, 193-202.
(16) Kim, Y.; Kim, E.; Clavier, G.; Audebert, P. New Tetrazine-Based Fluoroelectrochromic Window; Modulation of the Fluorescence Through Applied Potential. *Chem. Commun.* **2006**, 0, 3612-3614.
(17) Kuo, C. P.; Chuang, C. N.; Chang, C. L.; Leung, M. K.; Lian, H. Y.; Wu, K. C. W. White-Light Electrofluorescence Switching from Electrochemically Convertible Yellow and Blue Fluorescent Conjugated Polymers. *J. Mater. Chem. C* **2013**, *1*, 2121-2130.
(18) Wu, J. H.; Liou, G. S. High-Performance Electrofluorochromic Devices Based on Electrochromism and Photoluminescence-Active Novel Poly(4-Cyanotriphenylamine). *Adv. Funct. Mater.* **2014**, *24*, 6422-6429.
(19) Beneduci, A.; Cospito, S.; La Deda, M.; Chidichimo, G. Highly Fluorescent Thienoviologen-Based Polymer Gels for Single Layer Electrofluorochromic Devices. *Adv. Funct. Mater.* **2015**, *25*, 1240-1247.
(20) Xing, H.; Zhang, X.; Zhai, Q.; Li, J.; Wang, E. Bipolar Electrode Based Reversible Fluorescence Switch Using Prussian Blue/Au Nanoclusters Nanocomposite Film. Anal. Chem. **2017**, *89*, 3867-3872.
(21) Liu, J.; Shi, Y.; Wu, J.; Li, M.; Zheng, J.; Xu, C. Yellow Electrochromic Polymer Materials With Fine Tuning Electrofluorescences by Adjusting Steric Hindrance of Side Chains. RSC Adv. **2017**, *7*, 25444-25449.
(22) Santra, D. C.; Nad, S.; Malik, S. Electrochemical Polymerization of Triphenylamine End-Capped Dendron: Electrochromic and Electrofluorochromic Switching Behaviors. J. Electroanal. Chem. **2018**, *823*, 203-212.
(23) Cheng, S. W.; Han, T.; Huang, T. Y.; Tang, B. Z.; Liou, G. S. High-Performance Electrofluorochromic Devices Based on Aromatic Polyamides With AIE-Active Tetraphenylethene and Electro-Active Triphenylamine Moieties. Polym. Chem. **2018**, *9*, 4364-4373.
(24) Thelakkat, M. Star-Shaped, Dendrimeric and Polymeric Triarylamines as Photoconductors and Hole Transport Materials for Electro-Optical Applications. *Macromol. Mater. Eng.* **2002**, *287*, 442-461.
(25) Yen, H. J.; Liou, G. S. Solution-Processable Triarylamine-Based Electroactive High Performance Polymers for Anodically Electrochromic Applications. *Polym. Chem.* **2012**, *3*, 255-264.
(26) Yen, H. J.; Liou, G. S. Recent Advances in Triphenylamine-Based Electrochromic Derivatives and Polymers. *Polym. Chem.* **2018**, *9*, 3001-3018.
(27) Liu, H. S.; Pan, B. C.; Huang, D. C.; Kung, Y. R.; Leu, C. M.; Liou, G. S. Highly Transparent to Truly Black Electrochromic Devices Based on an Ambipolar System of Polyamides and Viologen. *NPG Asia Mater.* **2017**, 9, e388.
(28) Jennings, J. R.; Lim, W. Y.; Zakeeruddin, S. M.; Gratzel, M.; Wang, Q. A Redox-Flow Electrochromic Window. *ACS Appl. Mater. Interfaces* **2015**, *7*, 2827-2832.
(29) Wu, J. T.; Liou, G. S. A Novel Panchromatic Shutter Based on an Ambipolar Electrochromic System without Supporting Electrolyte. *Chem. Commun.* **2018**, *54*, 2619-2622.
(30) Leventis, N.; Chen, M. G.; Liapis, A. I.; Johnson, J. W.; Jain, A. Characterization of 3 x 3 Matrix Arrays of Solution-Phase Electrochromic Cells. *J. Electrochem. Soc.* **1998**, *145*, L55-L58.
(31) Ho, K. C.; Fang, Y. W.; Hsu, Y. C.; Chen, L. C. The Influences of Operating Voltage and Cell Gap on the Performance of a Solution-Phase Electrochromic Device Containing HV and TMPD. *Solid State Ionics* **2003**, *165*, 279-287.
(32) Hsiao, S. H.; Liou, G. S.; Kung, Y. C.; Yen, H. J. High Contrast Ratio and Rapid Switching Electrochromic Polymeric Films Based on 4-(Dimethylamino)triphenylamine-Functionalized Aromatic Polyamides. *Macromolecules* **2008**, *41*, 2800-2808.

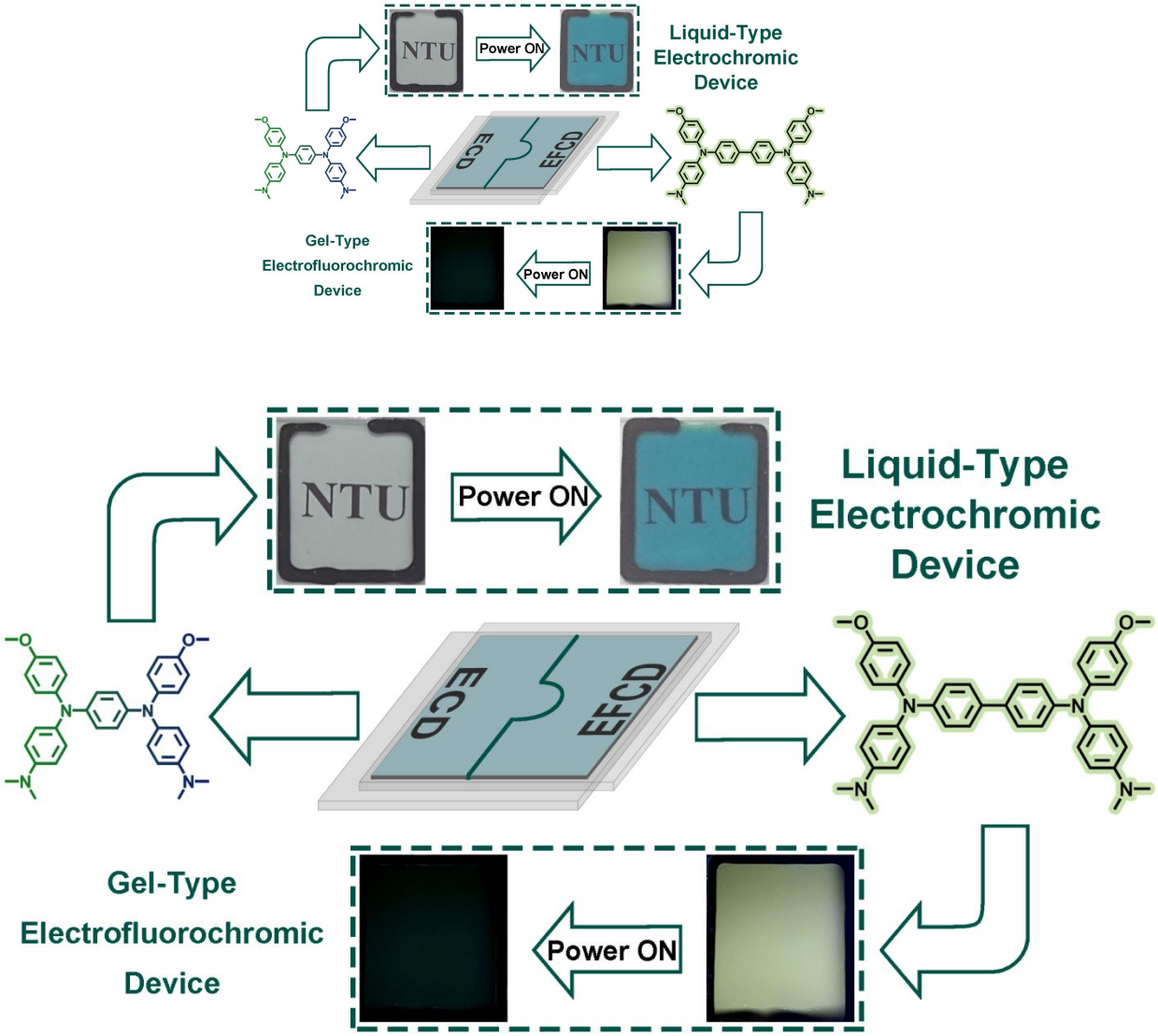
NTU
Power ON
NTU
Liquid-Type
Electrochromic
Device
ECD
EFCD
Gel-Type
Electrofluorochromic
Device
Power ON